Bulletin of Electrical Engineering and Informatics
Vol. 13, No. 2, April 2024, pp. 853∼864
ISSN: 2302-9285, DOI: 10.11591/eei.v13i2.5660

An enhanced control scheme for multifunctional grid connected PV system using fuzzy and predictive direct power control

Boualem Boukezata[1,2], Abdelmadjid Chaoui[2], Jean Paul Gaubert[3], Oussama Boutalbi[4]
[1]Department of Electronic, Faculty of Science and Technology, University Mohamed Elbachir El Ibrahimi of Bordj Bou Arreridj, Bordj Bou Arreridj, Algeria
[2]Laboratory of Power Quality in Electrical Networks (QUERE), Department of Electrical Engineering, Faculty of Technology, University of Ferhat Abbas Setif 1, Setif, Algeria
[3]Laboratory of Electrical Engineering and Automatic Control for Systems (LIAS), ENSIP, University of Poitiers, Poitiers, France
[4]Intelligent Systems Laboratory, Department of Electronic, Faculty of Technology, University of Ferhat Abbas Setif 1, Setif, Algeria

Article Info

Article history:

Received Dec 31, 2022
Revised Sep 11, 2023
Accepted Oct 16, 2023

Keywords:

Fuzzy logic control controller
Grid
Maximum power point tracking
Predictive direct power control
Photovoltaic system

ABSTRACT

This paper presents a combination between a fuzzy logic control (FLC) and a predictive direct power control for multifunctional grid connected photovoltaic (PV) system, to solve the oscillation problem in the DC link voltage of the inverter caused by the fast irradiation changing. The whole system consists of a PV system which interface a DC-AC inverter, a FLC maximum power point tracking (MPPT) algorithm has been adopted to operate the DC-DC converter at the MPP. The predictive control strategy is applied to the DC-AC inverter with FLC in its voltage control loop to improve the power exchange between the grid and the PV system. Simulation results have been verified through MATLAB/Simulink software for the purpose of giving the effectiveness of the suggested control against existed controllers.

Corresponding Author:

Boualem Boukezata
Department of Electronic, Faculty of Science and Technology
University Mohamed Elbachir El Ibrahimi of Bordj Bou Arreridj
Bordj Bou Arreridj, Algeria
Email: boualem.boukezata@univ-bba.dz

1. INTRODUCTION

Recently, with the rapid depletion of traditional sources of energy, renewable energy source has become the mainstream of industrial applications [1]. Among them, solar energy is the most promising one and has usually been in the best location to reduce the fossil fuel dependence in the energy industry [2], [3]. Particularly, photovoltaic (PV) power generation, is conducting to a fast growing integration of renewable energy sources as a distributed generation (DG) system into the utility grid. However, a large scale penetration of these sources poses serious problems, as it can threat the power system's stability and reliability [4]-[6]. Meanwhile, the main challenge of theses systems is the extraction of the maximum power of the PV system through maximum power point tracking (MPPT)s algorithms, as well as, the power quality injected to the grid, which is in direct relation with power converter and its control strategy [7], [8]. Therefore, the performance of theses systems is highly dependent on the choice of the power converter and the appropriate control technique [9]. The DC link capacitor voltage of the distributed DC-AC inverter should be controlled through a robust con-

trollers in order to enhance dynamics, which is prone to rapidly changing of climatic conditions as well as the power load variations. To cope with this problem, several control strategies have been reported in the literature [10]-[15]. Lu *et al.* [16] proposed an enhanced model predictive direct power control for a grid-connected converters where, two voltage vectors are applied over a control period and their duty to optimize the benefit of the PV owners and satisfy the limits of the voltage variations simultaneously. Krommydas and Alexandridis [17], a new approach of analysis is employed on the basis of nonlinear systems theory with purpose to develop an appropriate controllers with guaranteed stability. Researchers in [18], [19] propose an optimized direct power control and a predictive current control respectively in grid connected inverter combined with a PV system through PI controller to improve the power quality generation as well as the whole system stability under rapidly environmental conditions variation. Wu *et al.* [20] proposes a dc voltage droop control in the grid-connected photovoltaic system with a view to make the capacitance of the medium time scale contribute in the grid frequency response without any supplementary equipment. Zhou *et al.* [21] proposes a robust DC-link voltage control based on the linear active disturbance rejection control scheme to enhance the tolerance of PV grid-connected inverter to disturbances. In this work, fuzzy logic control as a robustness controller in predictive direct power control is suggested to enhance dynamics and provide a good quality of power to the grid in the presence of non linear load under all dynamic conditions. The purpose of this work is to propose a suitable direct power control (DPC) scheme combined with a robust fuzzy logic control (FLC) controller for the multi-functional grid-connected PV system based on a predictive approach. The principle of this approach is based on the selection of the optimal control vector to be applied during the sampling period. Where, the selection is done by optimizing a performance function. Moreover, in the dc link voltage control a FLC controller has been proposed to enhance the problem of PI controller under external disturbances (fast changing irradiance, non linear load variation).

2. SYSTEM DESCRIPTION

The schematic diagram of the multifunctional grid connected PV system with its control algorithm scheme is depicted in Figure 1. The PV system (part 1) consists of a PV panels, a DC-DC boost converter which is interfaced the DC link bus of the multifunctional inverter. A FLC MPPT algorithm is exploited to maximize power, and to provide pulses through PWM for controlling the DC-DC boost converter. The multifunctional inverter (part 2) is connected to the grid at the point of common coupling (PCC), which is controlled through a predictive direct power control via a FLC regulator in its voltage loop as depicted in the scheme of the control algorithm.

2.1. PV system

The PV array is designed in this paper for a 3600 W peak power tracking capacity. A solar PV module kyocera KC 200 W adopted in this work, the PV generator is composed of three strings, each string contains 6 panels. In order to interface the dc link voltage bus, the output voltage of the DC-DC converter must be very high. Hence, a DC-DC boost converter is necessary to offer high voltage gain as well as to reach the maximum power point via MPPT algorithm, the duty cycle D is the output of the MPPT algorithm which will be investigated to produce control signal for the switching metal oxide semiconductor field effect transistor (MOSFET). The PV system control scheme block is depicted in Figure 1 highlighted (part 1). The DC link voltage bus is given as (1):

$$V_{dc} = \frac{V_{pv}}{1 - D} \tag{1}$$

2.1.1. Maximum power point tracking fuzzy logic control

The investigation of fuzzy logic control has become more attractive during the last decade since it can deal with imprecise inputs, doesn't need any accurate mathematical model. Therefore, the application of FLC as a MPPT algorithm provides a good performance, where, the MPP tracking doesn't require any parameter information and consists of a step-wise adaptive search which leads to a rapid convergence [22]. This algorithm purposes to reach the MPP from the PV array whatever climatic conditions. The controller consists of three stages namely fuzzification, rules inference and defuzzification as presented in Figure 2.

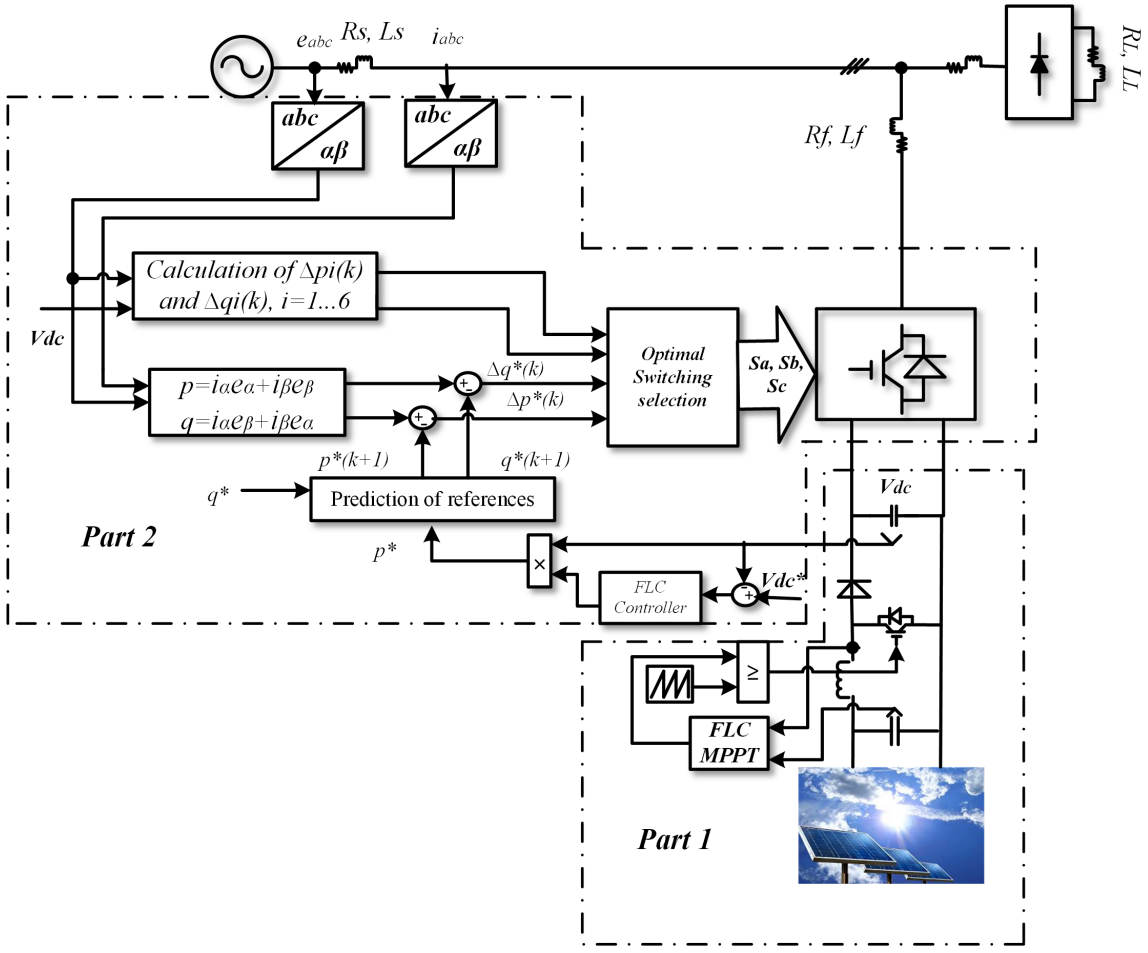

Figure 1. The schematic predictive DPC control of the whole system

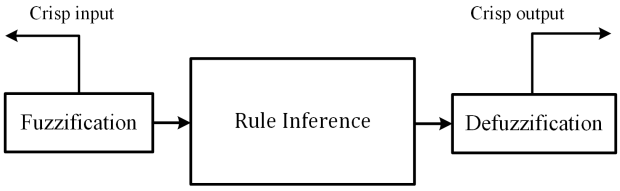

Figure 2. Structure of FLC

In this article, $\Delta p(k)$ and $\Delta v(k)$ are the input variables at each sampling time k of the proposed algorithm, the output variable is D which is the changing of the duty cycle. The variable $\Delta p(k)$ and $\Delta v(k)$ will be given as:

$$\Delta p(k) = p(k) - p(k-1)\ \Delta v(k) = v(k) - v(k-1)$$

where $p(k)$ is the PV array power and $v(k)$ is the PV array voltage. Thus, at the MPP $\Delta p(k)$ and $\Delta v(k)$ equal zero. Over fuzzification, the variables $\Delta p(k)$ and $\Delta v(k)$ are transferred into linguistic variables through a membership functions. The $\Delta p(k)$ and $\Delta v(k)$ universe of discourse are adopted to five fuzzy sets, including negative big (NB), negative small (NS), zero (ZE), positive small (PS), and positive big (PB) as depicted in Figure 3. Then, the output variable is developed based on rule base presented in Table 1.

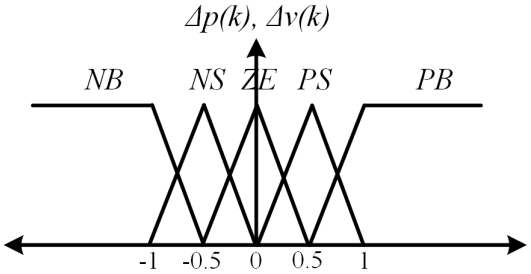

Figure 3. Membership functions of: $\Delta p(k)$, $\Delta v(k)$ and $\Delta(k+1)$

Table 1. Rule base table of FLC MPPT

		$\Delta v(k)$				
		NB	NS	ZE	PS	PB
$\Delta p(k)$	NB	PS	PB	PB	PB	NS
	NS	ZE	PS	PS	NS	ZE
	ZE	ZE	ZE	ZE	ZE	ZE
	PS	ZE	NS	NS	PS	ZE
	PB	NS	NB	NB	PB	PS

Mamdani fuzzy inference process is investigated with a fuzzy max-min operation in order to provide the fuzzy algorithm MPPT output. The obtained crisp is calculated in the defuzzification step via the center of gravity method. It computes the center of gravity of the final fuzzy crisp. The output value of the algorithm $\Delta D(k)$ is provided as (2):

$$\Delta D(k) = \frac{\sum_{i=0}^{n} W_i \Delta D_i}{\sum_{i=0}^{n} W_i} \tag{2}$$

where W_i is the weighting factor, n is the maximum number of effective rules and D_i is the value corresponding to the membership function of D. Finally, the duty cycle will be expressed as $D(k+1) = D(k) + \Delta D(k)$

2.2. Multifunctional inverter

2.2.1. Predictive direct power control

From Figure 4, the influence of filter and source resistors is omitted, the system equations are expressed as (3)-(5):

$$e - v_s = L_s \frac{di_s}{dt} \tag{3}$$

$$v_f - v_s = L_f \frac{di_f}{dt} \tag{4}$$

$$i_s + i_f = i_l \tag{5}$$

The purpose of the multifunctional system is for obtaining a sinusoidal current of the utility i_s, using the relationship 5. Assume that i_l can be expressed as (6):

$$i_l = i_{l,f} + i_{l,h} = i_s + i_f \tag{6}$$

where $i_{l,f}$ is the fundamental current and $i_{l,h}$ is the harmonics currents. Then, by manipulation in (6) can be exhibited as (7):

$$i_{l,f} - i_s = -\left(i_{l,h} - i_f\right) \quad \Rightarrow \quad \Delta i_s = -\Delta i_f \tag{7}$$

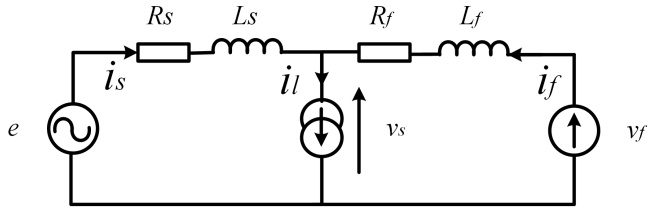

Figure 4. Schematic circuit of the multifunctional inverter

Based on the approximation $\Delta i = di$ for a small current variation; (7) will be expressed as (8):

$$di_s = -di_f \tag{8}$$

By subtracting (4) from (3) and substituting (5) in the result equation, we will obtain:

$$v_f - e = (L_f + L_s)\frac{di_f}{dt} \tag{9}$$

The obtained equation depicting the multifunctional inverter is presented as (10):

$$v_f - e = L\frac{di_f}{dt} \tag{10}$$

where $L = L_f + L_s$
In the stationary α-β reference frame and for a balanced three-phase system, the dynamics of the currents drawn by a multifunctional inverter [23], is given as (11):

$$\begin{cases} \frac{di_{f\alpha}}{dt} = \frac{1}{L}(e_\alpha - v_\alpha) \\ \frac{di_{f\beta}}{dt} = \frac{1}{L}(e_\beta - v_\beta) \end{cases} \tag{11}$$

From this equation, a discretization of the first order, over a switching period T_s, the components of the current vector at the end of the switching period are given by (12):

$$\begin{cases} \Delta i_\alpha = i_\alpha(k+1) - i_\alpha(k) = \frac{T_s}{L}(e_\alpha(k) - v_\alpha(k)) \\ \Delta i_\beta = i_\beta(k+1) - i_\beta(k) = \frac{T_s}{L}(e_\beta(k) - v_\beta(k)) \end{cases} \tag{12}$$

Furthermore, the instantaneous active and reactive powers are expressed by (13):

$$\begin{bmatrix} p \\ q \end{bmatrix} = \begin{bmatrix} e_\alpha & e_\beta \\ e_\beta & -e_\alpha \end{bmatrix} \begin{bmatrix} i_\alpha \\ i_\beta \end{bmatrix} \tag{13}$$

The sampling period T_s is supposed to be small in comparison with the period of the power-source voltage, components of $e_{\alpha\beta}$ are supposed constant during the switching period $e_\alpha(k) = e_\alpha(k+1)$. Consequently, the variation of active power Δp and reactive power Δq can be given as (14):

$$\begin{cases} \Delta p = e_\alpha(k) \cdot \Delta i_\alpha + e_\beta(k) \cdot \Delta i_\beta \\ \Delta q = e_\beta(k) \cdot \Delta i_\alpha + e_\alpha(k) \cdot \Delta i_\beta \end{cases} \tag{14}$$

Just seven variations can be realized on the active and reactive powers, by applying each of the seven control vectors over a switching period. These variations, named $\Delta p_i(k)$ and $\Delta q_i(k)$ are given by (15):

$$\begin{cases} \Delta p_i = \frac{T_a}{L}\left\|e_{\alpha\beta}(k)\right\|^2 - \frac{T_a}{L}\left\|e_{\alpha\beta}(k)\right\| \cdot [\cos(\theta)v_{\alpha i} + \sin(\theta)v_{\beta i}] \\ \Delta q_i = \frac{T_a}{L}\left\|e_{\alpha\beta}(k)\right\| \cdot [\cos(\theta)v_{\beta i} + \sin(\theta)v_{\alpha i}] \end{cases} \tag{15}$$

In normalized quantities these variations are expressed by (16):

$$\begin{cases} \overline{\Delta p_i} = \frac{\Delta p_i}{\frac{T_s}{L}\|e_{\alpha\beta}\|\|v_{\alpha\beta}\|} = \frac{\|e_{\alpha\beta}\|}{\|v_{\alpha\beta}\|} - [\cos(\theta)\bar{v}_{\alpha i} + \sin(\theta)\bar{v}_{\beta i}] \\ \overline{\Delta q_i} = \frac{\Delta q_i}{\frac{T_s}{L}\|e_{\alpha\beta}\|\|v_{\alpha\beta}\|} = \cos(\theta)\bar{v}_{\beta i} + \sin(\theta)\bar{v}_{\alpha i} \quad i = 0.1\ldots., 6 \end{cases} \tag{16}$$

The desired variations, $\Delta p_i(k)^*$ and $\Delta q_i(k)^*$, can be written in normalized quantities as (17):

$$\begin{cases} \overline{\Delta p_i}^* = \frac{\Delta p_i^*}{\frac{T_s}{L}\|e_{\alpha\beta}\|\|v_{\alpha\beta}\|} \\ \overline{\Delta q_i}^* = \frac{\Delta q_i^*}{\frac{T_s}{L}\|e_{\alpha\beta}\|\|v_{\alpha\beta}\|} \end{cases} \tag{17}$$

2.2.2. Prediction of instantaneous power references

The P-DPC needs the prediction of the instantaneous active and reactive power references at the next sampling time $p^*(k+1)$ and $q^*(k+1)$. Reference reactive power is frequently imposed zero for operation with a unitary power factor. The estimation of the reference of this power at the next sampling time $(k+1)$ is given as (18):

$$q^*(k+1) = q^*(k) \tag{18}$$

The active power command $p^*(k)$ is obtained from the FLC dc link voltage controller. If tracking error of dc link voltage is supposed constant during two successive sampling periods, the instantaneous active power command $p^*(k+1)$ can be estimated through a linear extrapolation as (19):

$$p^*(k+1) = 2p^*(k) - p^*(k-1) \tag{19}$$

2.2.3. Principle for selecting the optimal control vector

This predictive approach is based on the application of a single control vector at each switching period, which is similar to the DPC based on a predefined switching table, except that the control vector applied at this time is optimal. It corresponds to the most adequate variation among the seven possible variations described by (17). Once the desired variation $[\Delta pi(k), \Delta qi(k)]$ is calculated and normalized, the optimal control vector to be selected over the switching period $[kT_s, (k+1)T_s]$ corresponds to the variation point $\left[\overline{\Delta p_i}^*, \overline{\Delta q_i}^*\right]$ closest to the desired variation point. Then, the performance function to be optimized consists in searching for the smallest distance between the point $\left[\overline{\Delta p_i}^*, \overline{\Delta q_i}^*\right]$ and the points $[\Delta p_i(k), \Delta q_i(k)]$. It is formulated by the following objective (20) [24]:

$$f_i = \min\left(\sqrt{\left[\overline{\Delta p_i}^* - \Delta p_i\right]^2 - \left[\overline{\Delta q_i}^* - \Delta q_i\right]^2}\right) \quad i = 1, \ldots.6. \tag{20}$$

2.2.4. Fuzzy logic controller for DC link control

To elaborate the fuzzy logic controller, the input signals for this controller is the error of dc link voltage and its variation. While, its output signal is the variation of the maximum value of the current ΔI_{smax} as presented in Figure 5 [25].

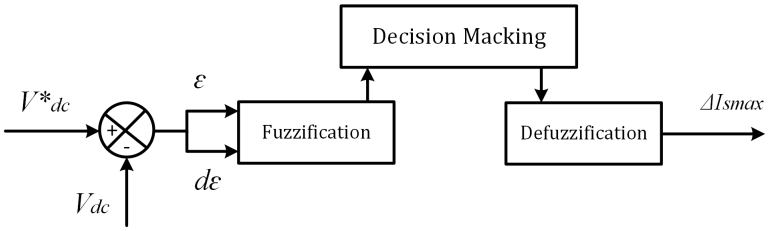

Figure 5. Schematics of dc link voltage regulation through FLC controller

The fuzzy controller is developed as: seven fuzzy sets for each input and output: negative big (NB), negative medium (NM), negative small (NS), zero (ZE), positive small (PS), positive medium (PM), positive big (PB). Mamdani method is employed with a fuzzy max-min operation. The membership functions of error (ϵ) and change in error ($d\epsilon$) of dc link voltage are shown in Figure 6.

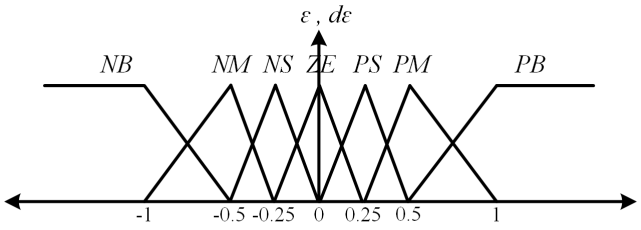

Figure 6. Normalized triangular membership functions

2.2.5. Design of rules table

The fuzzy control rules which relates the input variables to the output are presented in Table 2. The deffuzification process produces the single crisp value of output (ΔI_{smax}) from the aggregated fuzzy set which includes a range of output values. The commonly used centroid method is employed to transform the fuzzy subset of (ΔI_{smax}) to numerical value. It calculates the center of gravity from the obtained output fuzzy set, and provides the final result.

Table 2. Rule base table of FLC controller

		ϵ						
		NB	NM	NS	ZE	PS	PM	PB
	NB	NB	NB	NB	NB	NM	NS	ZE
	NM	NB	NB	NB	NM	NS	ZE	PP
	NS	NB	NB	NM	NS	ZE	PS	PM
$d\epsilon$	ZE	NB	NM	NS	ZE	PS	PM	PB
	PS	NM	NS	ZE	PS	PM	PB	PB
	PM	NS	ZE	PS	PM	PB	PB	PB
	PB	ZE	PS	PM	PB	PB	PB	PB

3. RESULTS AND DISCUSSION

The proposed predictive direct power control combined with FLC controllers was verified in simulation using MATLAB/Simulink. The topology of the simulated system is depicted in Figure 1 and the simulation parameters of the entire system are given in the Table 3. In order to illustrate the simulation steady and dynamic state to assess the effect of fast irradiation changing, a consecutive irradiation ramp evolution was adopted. This irradiation change starts from 0 W/m^2, stops at 350 W/m^2, waits at this level for 0.25 s, and then continue to increase again to 600 W/m^2 and 1000 W/m^2 respectively with a constant slope and stay at their levels during 1.5 s as depicted in Figure 7. The environmental temperature is assumed constant (25 °C) in all simulation test.

Table 3. PV array parameters

Parameters	Values
v_s, f_s	80 V, 50 Hz
L_s, R_s	0.1 mH, 0.1 Ω
L_l, R_l	10 mH, 20 Ω
L_f, R_f, C	1 mH, 0.01 Ω, 1100 μ F
L_c, R_c	0.55 mH, 0.01 Ω
$PVarray$	N_{pp}=3, N_{ss}=6

Figure 8 depicts waveforms of the source current, the load current and the filter current and their zoom at each ramp irradiation changing. Figures 9 and 10 show the power flows as well as the duty cycle of the dc dc boost converter. When the control is not activated with a G=0 W/m^2 between 0 s and 0.1 s, non linear load causes a serious problem of current harmonic and reactive current at the pcc exhibited by the waveform

of the source current and the reactive power supplied by the grid. When the predictive direct power control is switched on at t=0.1 s, the source current becomes sinusoidal improved by the injected filter current with a unity power factor. The source current THD decreased to 1.66% as shown in Figure 11, which is acceptable with IEEE Standard 519-1992.

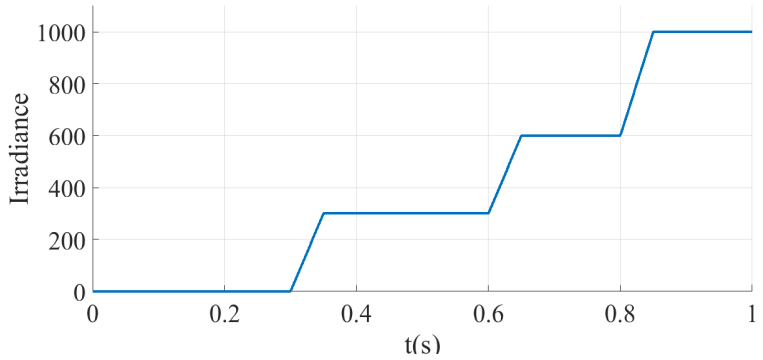

Figure 7. Profile of irradiance

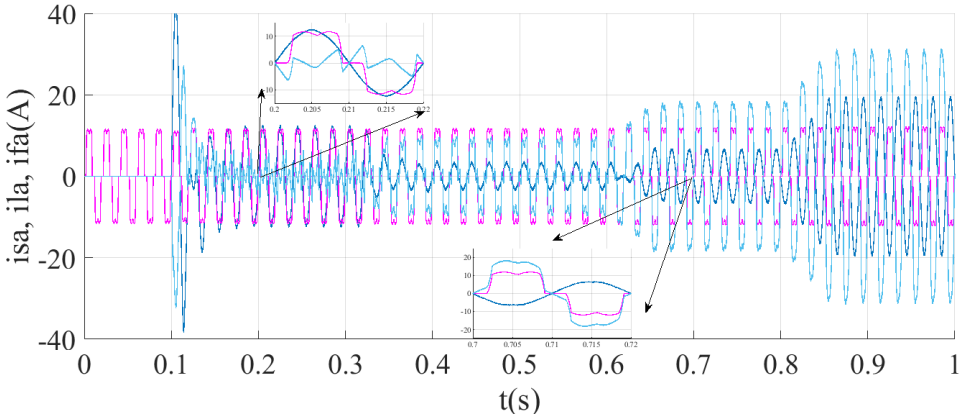

Figure 8. Waveforms of the whole system currents

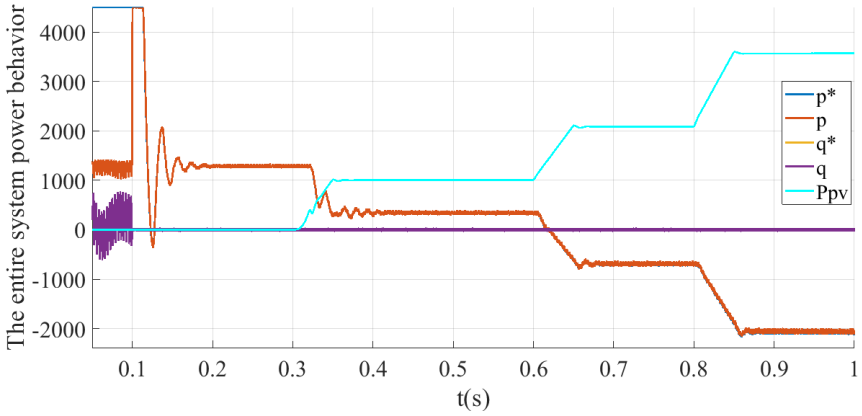

Figure 9. The entire system power behavior

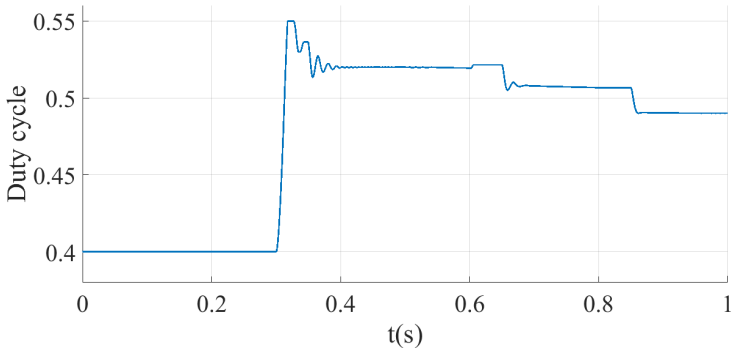

Figure 10. Duty cycle behavior

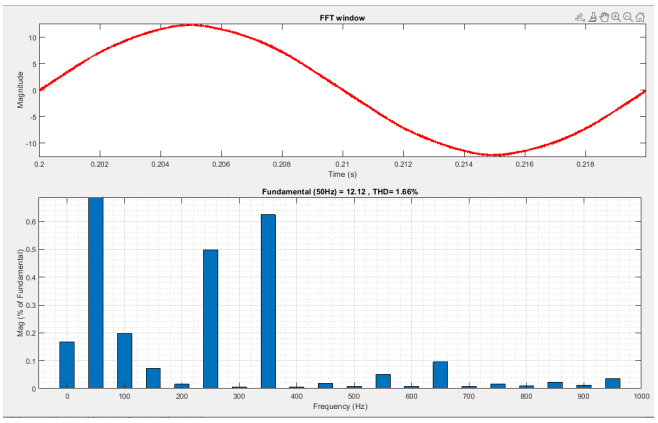

Figure 11. Grid current FFT

Furthermore, in the multifunctional PV system mode at t=0.3 s, an increase in the irradiation at 0.3 s gives rise a PV power generation, the PV system and the grid provides the required power demanded by the load. Thus, for each step irradiation changing at 0.6 s and 0.85 s respectively, the FLC MPPT algorithm provides a best tracking of PV power with a minimum oscillation; where there is no power loss in dynamic and steady state cases. For each PV power increase the active power fedded by the grid decreased until the multifunctional PV system supports all non linear load power demanded. The source current stays sinusoidal in phase with the voltage source whatever the irradiance variation, the THD level is reduced to 1.25%, as given in Figure 12.

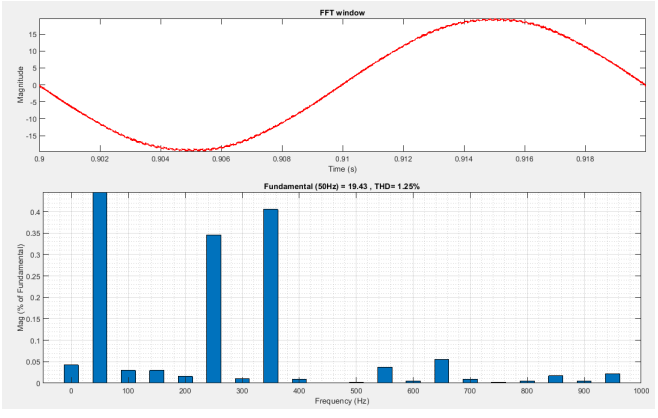

Figure 12. Grid current FFT

The dc link voltage follows its desired value 300 V at 0.1 s with a minimal overshoot as well as a rise time of 0.0015 s with FLC controller, and then for each step changing irradiation, the FLC controller proves more robustness and stability under fast irradiation changing; there is no overshoot just a little increase of DC link voltage then the controller can maintains it at its desired level, as shown in Figure 13. However; through PI controller; we show that the DC link voltage reaches its desired value before 0.165 s to reach 300 V with an overshoot of 28v. The same remark when the irradiation occurs at 0.3 s; 0.6 s and 0.8 s the increase in irradiation causes an increase in the dc link voltage with overshoot of 12.05 V then it reaches its level during 0.1 s.

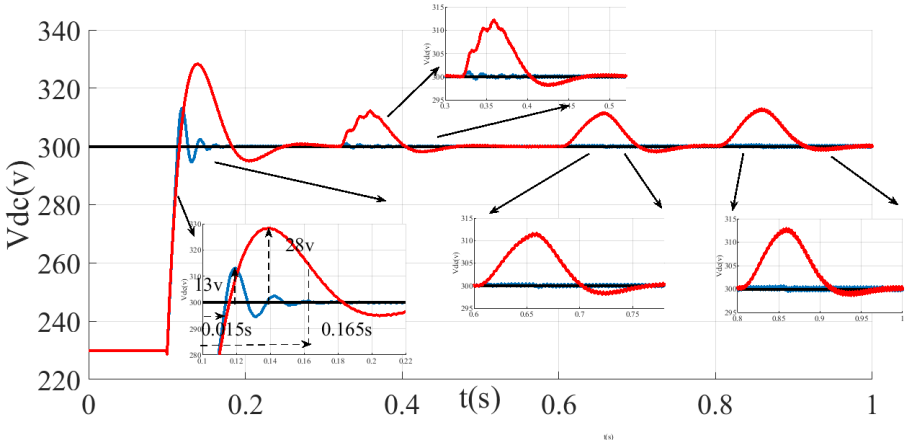

Figure 13. DC-link voltage behavior under ramp disturbances changing in solar irradiation

3.1. Comparative study between previously developped algorithms

Comparative study between previously developed algorithms is simulated with the same parameters of the proposed algorithm and is given in Table 4 under different irradiance conditions, specifically G=0 W/m² and G=1000 W/m². The THD levels are measured for each algorithm in both scenarios. In the case of Classical DPC, THD levels are recorded at 2.32% under no irradiance (G=0 W/m²) and 1.43% under irradiance (G=1000 W/m²). The Improved DPC algorithm shows notable improvement, with THD levels reduced to 1.46% and 1.3% under G=0 W/m² and G=1000 W/m², respectively. The proposed predictive DPC algorithm demonstrates competitive performance, yielding THD levels of 1.66% and 1.25% under the respective irradiance conditions.

Table 4. Comparative study of differents developped controls

Algorithms	THD level (%)	THD level (%)
	G=0	G=1000 W/m^2
Classical DPC	THD=2.32	THD=1.43
Improved DPC	THD=1.46	THD=1.3
Predictive DPC	THD=1.66	THD=1.25

4. CONCLUSION

Robust control algorithm in dc link voltage is very required in multifunctional grid connected PV system, which is directly affect the dynamic of the system. Therefore, a FLC controller with predictive direct power control was proposed in this system. A comparative study between direct power control algorithm with classical and new switching table and proposed predictive direct power algorithm have been verified in term of THD level. Simulation results confirm the superiority of the proposed controller against previously developed controllers.

ACKNOWLEDGEMENT

Authors thank the Ministry of Higher Education and Scientific Research of Algeria for providing financial support.

REFERENCES

[1] T. Vigneysh and N. Kumarappan, "Grid interconnection of renewable energy sources using multifunctional grid-interactive converters: A fuzzy logic based approach," *Electric Power Systems Research*, vol. 151, pp. 359–368, 2017, doi: 10.1016/j.epsr.2017.06.010.

[2] A. Safa, E. L. M. Berkouk, Y. Messlem, and A. Gouichiche, "A robust control algorithm for a multifunctional grid tied inverter to enhance the power quality of a microgrid under unbalanced conditions," *International Journal of Electrical Power & Energy Systems*, vol. 100, February, pp. 253–264, 2018, doi: 10.1016/j.ijepes.2018.02.042.

[3] M. A. Khan, A. Haque, V. S. B. Kurukuru, and S. Mekhilef, "Advanced Control Strategy With Voltage Sag Classification for Single-Phase Grid-Connected Photovoltaic System," *IEEE Journal of Emerging and Selected Topics in Industrial Electronics*, vol. 3, no. 2, 2020, doi: 10.1109/jestie.2020.3041704.

[4] M. B. Satti and A. Hasan, "Direct Model Predictive Control of Novel H-Bridge Multilevel Inverter Based Grid-Connected Photovoltaic System," *IEEE Access*, vol. 7, no. 1, pp. 62750–62758, 2019, doi: 10.1109/ACCESS.2019.2916195.

[5] A. Sabir and M. S. Javaid, "Robust Control of Grid-Connected Photovoltaic Systems Under Unbalanced Faults Without PLL," *Canadian Journal of Electrical and Computer Engineering*, vol. 41, no. 4, pp. 179–190, 2018, doi: 10.1109/CJECE.2018.2876609.

[6] R. Vieira, M. I. Guerra, and S. Bandeira, "Analysis of the Power Quality of a Grid-Connected Photovoltaic System," *IEEE Latin America Transactions*, vol. 18, no. 4, pp. 714–721, 2020, doi: 10.1109/TLA.2020.9082214.

[7] B. Singh, C. Jain, S. Goel, R. Gogia, and U. Subramaniam, "A Sustainable Solar Photovoltaic Energy System Interfaced with Grid-Tied Voltage Source Converter for Power Quality Improvement," *Electric Power Components System*, vol. 45, no. 2, pp. 171–183, 2017, doi: 10.1080/15325008.2016.1233298.

[8] R. K. Agarwal, I. Hussain, B. Singh, A. Chandra, and K. Al-Haddad, "A multifunctional three-phase grid-connected single-stage SPV system using an intelligent adaptive control technique," *IECON 2016 - 42nd Annual Conference of the IEEE Industrial Electronics Society*, pp. 3000–3005, 2016, doi: 10.1109/IECON.2016.7793465.

[9] A. Khandelwal and P. Nema, "Application of PI controller based active filter for harmonic mitigation of grid-connected PV-system," *Bulletin of Electrical Engineering and Informatics*, vol. 10, no. 5, pp. 2377–2383, 2021, doi: 10.11591/eei.v10i5.2907.

[10] S. H. Mohamad, M. A. M. Radzi, N. F. Mailah, N. I. A. Wahab, A. Jidin, and M. Y. Lada, "Adaptive notch filter under indirect and direct current controls for active power filter," *Bulletin of Electrical Engineering and Informatics*, vol. 9, no. 5, pp. 1794–1802, 2020, doi: 10.11591/eei.v9i5.2165.

[11] A. M. Hadi, E. M. Thajeel, and A. K. Nahar, "A novel optimizing PI control of shunt active power filter for power quality enhancement," *Bulletin of Electrical Engineering and Informatics*, vol. 11, no. 3, pp. 1194–1202, 2022, doi: 10.11591/eei.v11i3.3225.

[12] A. Chatterjee, K. Mohanty, V. S. Kommukuri, and K. Thakre, "Power quality enhancement of single phase grid tied inverters with model predictive current controller," *Journal Renewable Sustainable Energy*, vol. 9, no. 1, 2017, doi: 10.1063/1.4973714.

[13] S. Xu, R. Shao, B. Cao, and L. Chang, "Single-phase grid-connected PV system with golden section search-based MPPT algorithm," *Chinese Journal of Electrical Engineering*, vol. 7, no. 4, pp. 25–36, 2021, doi: 10.23919/CJEE.2021.000035.

[14] A. Datta, R. Sarker, and I. Hazarika, "An Efficient Technique Using Modified p–q Theory for Controlling Power Flow in a Single-Stage Single-Phase Grid-Connected PV System," *IEEE Transactions on Industrial Informatics*, vol. 15, no. 8, pp. 4635–4645, 2018, doi: 10.1109/tii.2018.2890197.

[15] A. M. Bozorgi, H. Gholami-Khesht, M. Farasat, S. Mehraeen, and M. Monfared, "Model Predictive Direct Power Control of Three-Phase Grid-Connected Converters with Fuzzy-Based Duty Cycle Modulation," *IEEE Transactions on Industry Applications*, vol. 54, no. 5, pp. 4875–4885, 2018, doi: 10.1109/TIA.2018.2839660.

[16] K. Lu, F. Lin, and B. Yang, "Profit Optimization-Based Power Compensation Control Strategy for Grid-Connected PV System," Br. J. Surg., vol. 106, no. 5, pp. 11–47, 2019, doi: 10.1002/bjs.11340.

[17] K. F. Krommydas and A. T. Alexandridis, "Nonlinear Analysis Methods Applied on Grid-Connected Photovoltaic Systems Driven by Power Electronic Converters," *IEEE Journal of Emerging and Selected Topics in Power Electronics*, vol. 8, no. 4, pp. 3293–3306, 2020, doi: 10.1109/JESTPE.2020.2992969.

[18] B. Boukezata, A. Chaoui, J. P. Gaubert, and M. Hachemi, "Power Quality Improvement by an Active Power Filter in Grid-connected Photovoltaic Systems with Optimized Direct Power Control Strategy," *Electric Power Components Systems*, vol. 44, no. 18, pp. 2036–2047, 2016, doi: 10.1080/15325008.2016.1210698.

[19] B. Boukezata, J.-P. Gaubert, A. Chaoui, and M. Hachemi, "Predictive current control in multifunctional grid connected inverter interfaced by PV system," *Solar Energy*, vol. 139, 2016, doi: 10.1016/j.solener.2016.09.029.

[20] F. Wu *et al.*, "Inertia and Damping Analysis of Grid-Tied Photovoltaic Power Generation System with DC Voltage Droop Control," *IEEE Access*, vol. 9, pp. 38411–38418, 2021, doi: 10.1109/ACCESS.2021.3059687.

[21] X. Zhou, Q. Liu, Y. Ma, and B. Xie, "DC-Link voltage research of photovoltaic grid-connected inverter using improved active disturbance rejection control," *IEEE Access*, vol. 9, pp. 9884–9894, 2021, doi: 10.1109/ACCESS.2021.3050191.

[22] L. Farah, A. Hussain, A. Kerrouche, C. Ieracitano, J. Ahmad, and M. Mahmud, "A highly-efficient fuzzy-based controller with high reduction inputs and membership functions for a grid-connected photovoltaic system," *IEEE Access*, vol. 8, pp. 163225–163237, 2020, doi: 10.1109/ACCESS.2020.3016981.

[23] B. Boukezata, A. Chaoui, J. P. Gaubert, and M. Hachemi, "An improved fuzzy logic control MPPT based P&O method to solve fast irradiation change problem," *Journal Renewable Sustainable Energy*, vol. 8, no. 4, Jul. 2016, doi: 10.1063/1.4960409.

[24] A. Bouafia, J. -P. Gaubert and F. Krim, "Predictive Direct Power Control of Three-Phase Pulsewidth Modulation (PWM) Rectifier Using Space-Vector Modulation (SVM)," *IEEE Transactions on Power Electronics*, vol. 25, no. 1, pp. 228-236, 2010, doi: 10.1109/TPEL.2009.2028731.

[25] I. Colak, R. Bayindir, O. Kaplan and F. Tas, "DC Bus Voltage Regulation of an Active Power Filter Using a Fuzzy Logic Controller," *2010 Ninth International Conference on Machine Learning and Applications*, 2010, pp. 692-696, doi: 10.1109/ICMLA.2010.165.

BIOGRAPHIES OF AUTHORS

Boualem Boukezata was born in Setif, Algeria, on December 23, 1987. He received the Master and Ph.D. degrees in Electrical Engineering from the University of Setif 1, in 2011 and 2017, respectively. He is currently an assistant professor at the Electronic Department, University of Mohamed Elbachir El Ibrahimi, Bordj Bou Arreridj, Algeria. His main research interests are analysis, simulation, and design of power converters, circuit and systems for renewable energy sources, and power quality systems (active power filters). He can be contacted at email: boualem.boukezata@univ-bba.dz.

Abdelmadjid Chaoui was born in Algeria in 1968. He received the Engineering and Master's degrees in electrical engineering from Setif University, Algeria, in 1990 and 1996 respectively. In 2010, He obtained the Ph.D. degree in Power Electronic and Control from Setif and Poitiers Universities, Algeria and France respectively. He is currently an assistant Member Professor at the Department of Electrical Engineering, University of Setif 1, Algeria. Member of Power Electronic and Industrial Control Laboratory, Setif 1 University. His main research interests are power electronics control applied to renewable energy and power quality systems. He can be contacted at email: abdelmadjid.chaoui@univ-setif.dz.

Jean Paul Gaubert he received the Engineer's degree from the University of Clermont-Ferrand, France, in 1988, the M.Sc. and the Ph.D. degrees from the University of Science and Technology of LILLE, France, in 1990 and 1992, respectively, all in Electrical Engineering. He is actually Full Professor at Poitiers University, Poitiers, France, and a member of the Electrical Engineering and Automatic Control for Systems Laboratory (LIAS) of Poitiers. His current research interests are modeling and advanced control of power converters and power electronics systems and their digital control techniques. The derived topics deal with power quality such as active power filters, PWM rectifiers, interfacing renewable energy systems or optimal management of electrical micro-grids. He is a member of IEEE and EPE association. He can be contacted at email: jean.paul.gaubert@univ-poitiers.fr.

Oussama Boutalbi was born in 1988 Setif, Algeria. He has received Engineer, Master and Ph.D. degrees from Ferhat Abbas Setif1 University, in 2010, 2014 and 2020 respectively. Since 2013 he is with Intelligent Systems Laboratory (LSI), Electronic department Ferhat Abbas Setif1 University. His research interests are: the motion planning and tracking control design of autonomous robotic systems, optimization and parameters identification, robust and adaptive control design for non-linear systems and the application of artificial intelligence techniques (deep learning, type 2 fuzzy logic and neural networks) for interactive motion of robotic systems. He can be contacted at email: botalbioussama@gmail.com.